

# Dicopper(II) Complexes with the Enantiomers of a Bidentate Chiral Reduced Schiff Base: Inclusion of Chlorinated Solvents and Chiral Recognition of 1,2-Dichloroethane Rotamers in the Crystal Lattice

Vamsee Krishna Muppidi<sup>[a]</sup> and Samudranil Pal<sup>\*[a]</sup>

**Keywords:** Dicopper(II) complexes / Chiral reduced Schiff Bases / Crystal structures / Chlorinated solvents / Enantioselective inclusion

Bisphenoxo-bridged dicopper(II) complexes  $[\text{Cu}_2\text{L}^n\text{Cl}_2]$  (**1** ( $n = 1$ ) and **2** ( $n = 2$ )) with the N,O-donor reduced Schiff bases *N*-(2-hydroxybenzyl)-(*R*)- $\alpha$ -methylbenzylamine ( $\text{HL}^1$ ) and *N*-(2-hydroxybenzyl)-(*S*)- $\alpha$ -methylbenzylamine ( $\text{HL}^2$ ) have been synthesised and characterised. In both **1** and **2**, the bidentate chiral ligands coordinate the metal centres through the secondary amine N atom and the bridging phenolate O atom. The chloride ion occupies the fourth coordination site and completes a slightly distorted square-planar  $\text{NO}_2\text{Cl}$  environment around each copper(II) centre. Magnetic susceptibility measurements in the solid state suggest a strong antiferromagnetic interaction between the metal centres in both complexes. Both **1** and **2** readily form 1:1 host-guest compounds with chlorinated solvents such as  $\text{CH}_2\text{Cl}_2$ ,  $\text{CHCl}_3$  and  $\text{Cl}(\text{CH}_2)_2\text{Cl}$ . All the host-guest compounds crystallise in

noncentrosymmetric space groups. **1**· $\text{CH}_2\text{Cl}_2$  and **2**· $\text{CH}_2\text{Cl}_2$  crystallise in the  $P2_1$  space group while **1**· $\text{CHCl}_3$ , **2**· $\text{CHCl}_3$ , **1**· $\text{Cl}(\text{CH}_2)_2\text{Cl}$  and **2**· $\text{Cl}(\text{CH}_2)_2\text{Cl}$  crystallise in the  $P2_12_12_1$  space group. In these inclusion crystals, the C–H...Cl interactions between the guest and the host molecules are primarily responsible for enclathration of the chloroalkane molecules. In the case of  $\text{CH}_2\text{Cl}_2$ , one of its Cl atoms acts as the acceptor. On the other hand, for  $\text{CHCl}_3$  and  $\text{Cl}(\text{CH}_2)_2\text{Cl}$ , the metal coordinated Cl atom of the host complex acts as the acceptor. The structures of **1**·(*P*)- $\text{Cl}(\text{CH}_2)_2\text{Cl}$  and **2**·(*M*)- $\text{Cl}(\text{CH}_2)_2\text{Cl}$  provide rare examples for chiral recognition of the right handed (*P*) and the left handed (*M*) gauche forms of  $\text{Cl}(\text{CH}_2)_2\text{Cl}$  in molecular assemblies.

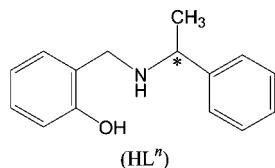
(© Wiley-VCH Verlag GmbH & Co. KGaA, 69451 Weinheim, Germany, 2006)

## Introduction

Materials generated by noncentrosymmetric organisation of molecules in the crystalline state are of current interest because of their potential applications in a variety of research areas such as enantioselective separation, asymmetric catalysis, drug delivery, non-linear optical effects and ferro-, pyro- and piezoelectricity.<sup>[1,2]</sup> The general strategy for noncentrosymmetric organisation in the crystal lattice is insertion of chirality in the molecule.<sup>[3]</sup> Synthesis and structures of some coordination complexes with chiral Schiff bases and their nonlinear optical properties have been reported recently.<sup>[4]</sup> Compared to the Schiff bases the reduced Schiff bases with the  $-\text{CH}_2-\text{NH}-$  backbone are considered to be conformationally more flexible. In coordination complexes with reduced Schiff bases, the increased acidity of the N–H fragment resulting from metal coordination is also expected to facilitate its participation in intermolecular hydrogen bonding interactions.<sup>[5]</sup> Introduction of chirality to such metal coordinated reduced Schiff bases often leads to novel metal–organic frameworks through intermolecular

noncovalent interactions.<sup>[5,6]</sup> Complexes of this type have shown the potential for applications in DNA cleavage activity and asymmetric catalysis.<sup>[6e,f]</sup> Recently we have reported two mononuclear square-pyramidal copper(II) complexes of the general formula  $[\text{Cu}(\text{L}^n\text{NO}_2)_2(\text{H}_2\text{O})]$  with the N,O-donor chiral reduced Schiff bases *N*-(2-hydroxy-5-nitrobenzyl)-(*R*)- $\alpha$ -methylbenzylamine  $\{(R)\text{-}2(\text{OH})\text{-}5\text{-}(\text{NO}_2)\text{-C}_6\text{H}_3\text{CH}_2\text{NHCH}(\text{CH}_3)\text{C}_6\text{H}_5, \text{HL}^1\text{NO}_2\}$  and *N*-(2-hydroxy-5-nitrobenzyl)-(*S*)- $\alpha$ -methylbenzylamine  $\{(S)\text{-}2(\text{OH})\text{-}5\text{-}(\text{NO}_2)\text{-C}_6\text{H}_3\text{CH}_2\text{NHCH}(\text{CH}_3)\text{C}_6\text{H}_5, \text{HL}^2\text{NO}_2\}$ . The complexes crystallise in the noncentrosymmetric space group *C2* with  $\text{Cl}(\text{CH}_2)_2\text{Cl}$  molecules as the guests. The crystal packing of these 1:1 inclusion compounds revealed intermolecular hydrogen-bonding-assisted, perfectly polar alignment of both host and guest molecules as well as enantioselective confinement of the chiral rotamers of  $\text{Cl}(\text{CH}_2)_2\text{Cl}$ .<sup>[7]</sup> In the present work, we report the synthesis and characterisation of the enantiomeric pair of bisphenoxo-bridged dicopper(II) complexes  $[\text{Cu}_2\text{L}^1\text{Cl}_2]$  (**1**) and  $[\text{Cu}_2\text{L}^2\text{Cl}_2]$  (**2**) with  $\text{HL}^n$ , the unsubstituted analogues of  $\text{HL}^n\text{NO}_2$ . Both **1** and **2** are found to be very good hosts to confine chloroalkanes [ $\text{CH}_2\text{Cl}_2$ ,  $\text{CHCl}_3$  and  $\text{Cl}(\text{CH}_2)_2\text{Cl}$ ] and to isolate the enantiopure chiral rotamers of  $\text{Cl}(\text{CH}_2)_2\text{Cl}$  in the noncentrosymmetric crystal lattice through intermolecular C–H...Cl interactions.

[a] School of Chemistry, University of Hyderabad, Hyderabad 500046, India  
Fax: +91-40-2301-2460  
E-mail: spsc@uohyd.ernet.in



## Results and Discussion

### Synthesis and Some Properties

The chiral reduced Schiff bases *N*-(2-hydroxybenzyl)-(*R*)- $\alpha$ -methylbenzylamine (HL<sup>1</sup>) and *N*-(2-hydroxybenzyl)-(*S*)- $\alpha$ -methylbenzylamine (HL<sup>2</sup>) were synthesised in about 75% yield by condensation of salicylaldehyde with the corresponding  $\alpha$ -methylbenzylamine (*R* or *S*) in methanol followed by reduction with NaBH<sub>4</sub>.<sup>[5,7]</sup> The elemental analysis and the spectroscopic data (IR and <sup>1</sup>H NMR) for HL<sup>1</sup> and HL<sup>2</sup> are very similar and consistent with the expected molecular formula and structure. The reactions of these reduced Schiff bases (HL<sup>n</sup>) with CuCl<sub>2</sub>·2H<sub>2</sub>O (1:1 mol ratio) in methanol provided the dark brown complexes **1** (*n* = 1) and **2** (*n* = 2) in about 60% yield. The elemental analysis data for **1** and **2** are consistent with the empirical formula CuL<sup>n</sup>Cl. In solutions, the complexes are electrically non-conducting in nature. Thus in each complex the metal ions are in the +2 oxidation state and the chloride ions are coordinated to the metal centres.

The IR spectra of **1** and **2** are very similar. A sharp band observed at 3245 cm<sup>-1</sup> is assigned to the secondary amine N–H group of the ligands. Several weak bands are observed in the range 2800–3050 cm<sup>-1</sup>. These are possibly due to the aromatic and aliphatic C–H stretches. The absence of any band near 3400 cm<sup>-1</sup> indicates the deprotonation of the phenolic OH of the bidentate ligands in both complexes. Thus, it is very likely that in each complex the metal ions are coordinated to the bridging phenoxo groups and the secondary amine N atoms of the two ligands. The remaining fourth coordination site of each metal ion is occupied by the chloride ion. X-ray structures (vide infra) confirm this type of coordination of the metal ions by the deprotonated reduced Schiff bases and the chloride ions in **1** and **2**.

The electronic spectral features of both complexes in chloroform solutions are essentially identical. A weak absorption observed near 650 nm is followed by three strong absorptions in the range 430–268 nm. The absorption at 650 nm is assigned to the d-d transition. The occurrence of this weak absorption in this region is consistent with square-based coordination geometry around the metal centre.<sup>[8]</sup> The intense absorptions at higher energy are most likely from the ligand-to-metal charge transfer and intraligand transitions.

### Magnetic Properties

Room temperature (300 K) magnetic moments of **1** and **2** in the powder phase are 1.10 and 1.11  $\mu_B$ , respectively. These values suggest a strong antiferromagnetic spin coupling

between the metal centres in each of the two complexes. In similar bisphenoxo-bridged dicopper(II) complexes, strong to very strong antiferromagnetic spin coupling is very common. The magnitude of the coupling constant *J* varies from –145 to –429 cm<sup>-1</sup> in this type of species.<sup>[9,10]</sup> To quantify the extent of antiferromagnetic spin coupling in the present complexes we have collected the magnetic susceptibility data of **1** in the temperature range 300–18 K at a fixed magnetic field of 5 kG. On cooling the magnetic moment gradually decreases and reaches a value of 0.20  $\mu_B$  at 18 K. The nature of the curve obtained by plotting the  $\mu_{\text{eff}}$  against *T* is typical for two antiferromagnetically coupled copper(II) centres (Figure 1). The data were analysed using the Bleany–Bowers expression<sup>[11]</sup> for  $\chi_M$  versus *T* derived from the isotropic spin-exchange Hamiltonian  $H = -2JS_1 \cdot S_2$ , where  $S_1 = S_2 = 1/2$ . The best least-squares fit<sup>[12]</sup> was obtained with  $g = 1.93(2)$ ,  $J = -307(2)$  cm<sup>-1</sup>, *p* (paramagnetic impurity with  $S = 1/2$ ) = 0.5% and TIP (temperature independent paramagnetism) =  $1.2 \times 10^{-4}$  emu mol<sup>-1</sup> (Figure 1).

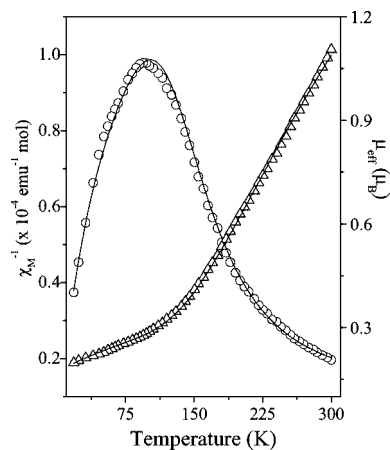


Figure 1. Temperature dependence of the inverse molar magnetic susceptibilities (O) and the effective magnetic moments ( $\Delta$ ) of [Cu<sub>2</sub>L<sup>1</sup><sub>2</sub>Cl<sub>2</sub>] (**1**); the solid lines were generated from the best least-squares fit parameters given in the text.

### Molecular Structures of **1** and **2**

X-ray structures of very few bisphenoxo-bridged dicopper(II) complexes of formula [Cu<sub>2</sub>L<sub>2</sub>X<sub>2</sub>] (L = monoanionic bridging N,O-donor ligand and X = halide) are known.<sup>[10]</sup> All these complexes are with achiral Schiff bases and they crystallise in centrosymmetric space groups with the monomeric unit in the asymmetric unit. The Cu<sub>2</sub>O<sub>2</sub> core is perfectly planar as the crystallographic inversion centre sits at the centre of the dimeric structure. For the same reason the X–Cu...Cu–X torsion angles are exactly 180° indicating a perfect trans orientation of the metal coordinated halides. In contrast, the host-guest compounds of both **1** and **2** crystallise in noncentrosymmetric space groups as they contain chiral ligands. In each case, the asymmetric unit contains a

complete dimeric complex molecule. Representative molecular structures of **1** and **2** are depicted in Figure 2 and the bond parameters associated with the metal ions for all the structures are listed in Table 1. The  $\text{NO}_2\text{Cl}$  coordination sphere around each metal centre is constituted by the secondary amine N atom, two bridging phenoxo groups and the chloride ion. The metal to coordinating atom bond lengths are essentially identical in all the structures and they are comparable with the values reported for copper(II) species having the same coordinating atoms.<sup>[7,9,10]</sup> In the N,O-donor reduced Schiff bases, HL<sup>1</sup> and HL<sup>2</sup>, the chiral C centre has the absolute configuration *R* or *rectus* and *S* or *sinister*, respectively. After complexation with the metal ion the N atom of the deprotonated monoanionic ligand becomes chiral. In **1**, the absolute configuration of the N centre is found to be *S* while in **2**, it is found to be *R*. Thus the generation of the new chiral centre is heterogeneous in both cases. As expected, the structures of **1** and **2** are mirror images of each other (Figure 2). In all the structures, the geometrical parameters for the  $\text{Cu}_2\text{N}_2\text{O}_2\text{Cl}_2$  fragment are very similar. The  $\text{NO}_2\text{Cl}$  coordination sphere around each metal centre is not exactly square planar. The Cl atoms deviate significantly from the  $\text{NO}_2$  plane. The deviation of Cl2 [1.198(8)–1.385(5) Å] is noticeably larger than that of Cl1

[0.674(9)–0.876(7) Å] (Figure 2). There is a relatively marginal deviation of the metal centre (0.05–0.09 Å for Cu1 and 0.15–0.21 Å for Cu2) from the  $\text{NO}_2$  plane. The  $\text{Cu}_2\text{O}_2$  core is also not planar in any of the structures; it is folded along the O···O line. The fold angles are in the range 18.61(9)–21.02(13)°. However, the solid angles (358.34–359.99°) indicate that the bridging phenoxide O atoms have essentially no pyramidal character. The Cu–O–Cu bridge angles and the Cu···Cu distances are in the ranges 100.01(12)–103.17(12)° and 3.0198(8)–3.0280(8) Å, respectively. Unlike the previously known structures of analogous dicopper(II) complexes,<sup>[10]</sup> the metal coordinated chlorides are not trans orientated in the present structures (Figure 2). Here the Cl1–Cu1···Cu2–Cl2 torsion angles are in the range 105–112°. Although the  $\text{Cu}_2\text{N}_2\text{O}_2\text{Cl}_2$  fragments are very similar in all the structures, the overall molecular conformations of the dicopper(II) complexes differ to some extent in the adducts of  $\text{CH}_2\text{Cl}_2$  compared to the very similar conformations in the adducts of  $\text{CHCl}_3$  and  $\text{Cl}(\text{CH}_2)_2\text{Cl}$ . The difference arises primarily from the variation in the orientation of the phenyl ring of the  $\alpha$ -methylbenzylamine fragment of the chiral bidentate ligands. The overlay diagrams of the dicopper(II) complex molecules **1** and **2** in all the inclusion compounds are shown in Figure 3.

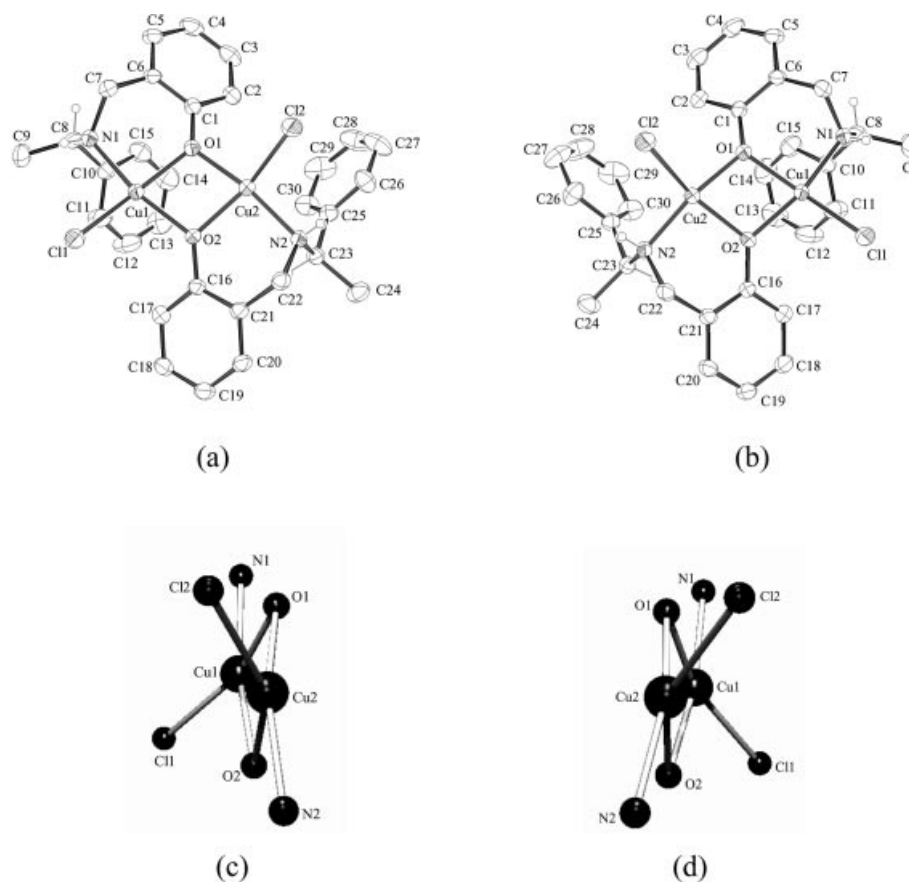
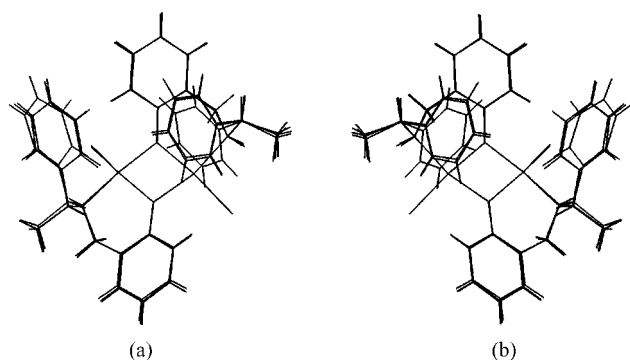


Figure 2. Molecular structures of (a)  $[\text{Cu}_2\text{L}^1_2\text{Cl}_2]$  (**1**) and (b)  $[\text{Cu}_2\text{L}^2_2\text{Cl}_2]$  (**2**) with the atom-labelling scheme; all non-hydrogen atoms are represented by their 30% probability thermal ellipsoids; except the hydrogen atoms on the chiral centres all other hydrogen atoms are omitted for clarity; the ball-stick representations of the  $\text{Cu}_2\text{N}_2\text{O}_2\text{Cl}_2$  units in (c) **1** and (d) **2**.

Table 1. Selected bond lengths [ $\text{\AA}$ ] and angles [ $^\circ$ ] for **1**·CH<sub>2</sub>Cl<sub>2</sub>, **1**·CHCl<sub>3</sub>, **1**·Cl(CH<sub>2</sub>)<sub>2</sub>Cl, **2**·CH<sub>2</sub>Cl<sub>2</sub>, **2**·CHCl<sub>3</sub> and **2**·Cl(CH<sub>2</sub>)<sub>2</sub>Cl.

Compound	<b>1</b> ·CH <sub>2</sub> Cl <sub>2</sub>	<b>1</b> ·CHCl <sub>3</sub>	<b>1</b> ·Cl(CH <sub>2</sub> ) <sub>2</sub> Cl	<b>2</b> ·CH <sub>2</sub> Cl <sub>2</sub>	<b>2</b> ·CHCl <sub>3</sub>	<b>2</b> ·Cl(CH <sub>2</sub> ) <sub>2</sub> Cl
Cu(1)–O(1)	1.944(2)	1.944(3)	1.938(3)	1.941(3)	1.942(3)	1.939(3)
Cu(1)–O(2)	1.965(2)	1.985(3)	1.975(3)	1.964(2)	1.980(3)	1.979(3)
Cu(1)–N(1)	1.993(3)	2.011(4)	2.004(4)	1.991(3)	2.010(4)	2.000(4)
Cu(1)–Cl(1)	2.2108(11)	2.2176(13)	2.2129(14)	2.2090(12)	2.2164(13)	2.2126(13)
Cu(1)–Cu(2)	3.0238(5)	3.0280(8)	3.0252(9)	3.0240(6)	3.0266(7)	3.0198(8)
Cu(2)–O(1)	1.920(2)	1.922(3)	1.926(3)	1.920(3)	1.921(3)	1.924(3)
Cu(2)–O(2)	1.963(2)	1.954(3)	1.961(3)	1.959(3)	1.951(3)	1.962(3)
Cu(2)–N(2)	1.967(3)	1.970(4)	1.979(4)	1.966(3)	1.971(4)	1.971(3)
Cu(2)–Cl(2)	2.2102(10)	2.2189(14)	2.2190(14)	2.2105(11)	2.2172(14)	2.2141(13)
O(1)–Cu(1)–O(2)	76.65(10)	76.07(12)	76.44(14)	76.50(10)	75.95(12)	76.65(12)
O(1)–Cu(1)–N(1)	91.53(11)	91.00(16)	91.22(16)	91.56(13)	91.05(15)	91.42(15)
O(2)–Cu(1)–N(1)	167.41(11)	166.79(16)	166.95(16)	167.19(13)	166.66(16)	167.28(15)
O(1)–Cu(1)–Cl(1)	161.45(9)	164.92(12)	165.03(13)	161.51(10)	164.82(12)	164.96(13)
O(2)–Cu(1)–Cl(1)	100.40(8)	100.47(10)	100.46(11)	100.59(9)	100.62(10)	100.48(10)
N(1)–Cu(1)–Cl(1)	92.19(9)	92.72(14)	92.55(13)	92.20(11)	92.72(14)	92.18(12)
O(1)–Cu(2)–O(2)	77.24(10)	77.30(13)	77.06(14)	77.08(10)	77.11(12)	77.41(12)
O(1)–Cu(2)–N(2)	165.17(12)	167.55(17)	166.33(18)	165.14(12)	167.27(17)	166.49(17)
O(2)–Cu(2)–N(2)	93.25(11)	93.15(15)	92.89(15)	93.28(11)	93.26(15)	92.60(14)
O(1)–Cu(2)–Cl(2)	98.70(8)	97.85(11)	98.30(12)	98.75(9)	97.92(10)	98.05(11)
O(2)–Cu(2)–Cl(2)	153.36(9)	155.40(12)	156.12(12)	153.55(10)	155.59(12)	156.46(12)
N(2)–Cu(2)–Cl(2)	94.84(9)	94.12(13)	94.59(12)	94.85(10)	94.25(13)	94.69(12)
Cu(1)–O(1)–Cu(2)	102.98(11)	103.09(13)	103.02(17)	103.09(11)	103.17(12)	102.84(13)
Cu(1)–O(2)–Cu(2)	100.69(11)	100.50(14)	100.44(15)	100.85(11)	100.67(13)	100.01(12)

Figure 3. Overlay diagrams of (a) the molecules of [Cu<sub>2</sub>L<sub>1</sub><sup>2</sup>Cl<sub>2</sub>] (**1**) and (b) the molecules of [Cu<sub>2</sub>L<sub>2</sub><sup>2</sup>Cl<sub>2</sub>] (**2**) in the host-guest crystals with CH<sub>2</sub>Cl<sub>2</sub>, CHCl<sub>3</sub> and Cl(CH<sub>2</sub>)<sub>2</sub>Cl.

### Host-Guest Interactions

Attempts to grow single crystals of both **1** and **2** revealed that the host lattices formed by these enantiomeric complexes have considerable structural adaptability to accommodate a range of chlorinated solvents such as CH<sub>2</sub>Cl<sub>2</sub>, CHCl<sub>3</sub> and Cl(CH<sub>2</sub>)<sub>2</sub>Cl. In all the cases, 1:1 host-guest crystals have been isolated. The host-guest crystals involving CH<sub>2</sub>Cl<sub>2</sub> crystallise in the monoclinic *P*2<sub>1</sub> space group while the other host-guest crystals involving CHCl<sub>3</sub> and Cl(CH<sub>2</sub>)<sub>2</sub>Cl crystallise in the orthorhombic *P*2<sub>1</sub>2<sub>1</sub>2<sub>1</sub> space group. Both space groups are noncentrosymmetric. In each case, the asymmetric unit contains one dicopper(II) complex molecule and one chloroalkane molecule. Recently, there have been several reports on the propensity of the Cl atom of C–Cl and M–Cl moieties to act as an acceptor in intermolecular hydrogen bonding interactions.<sup>[13]</sup> The crystal structures described here provide examples for both C–H···Cl–C and C–H···Cl–Cu hydrogen bonding interactions

involving the host and guest molecules. The geometrical parameters associated with the observed C–H···Cl interactions are listed in Table 2.

Table 2. Geometrical parameters for intermolecular hydrogen bonds.

Compound	D···A	<i>d</i> <sub>(D···A)</sub> [ $\text{\AA}$ ]	D–H···A [ $^\circ$ ]
<b>1</b> ·CH <sub>2</sub> Cl <sub>2</sub>	C(11)···Cl(3)	3.444(7)	132
	C(22)···Cl(4)	3.726(4)	161
<b>2</b> ·CH <sub>2</sub> Cl <sub>2</sub>	C(11)···Cl(3)	3.451(8)	134
	C(22)···Cl(4)	3.724(4)	161
<b>1</b> ·CHCl <sub>3</sub>	C(31)···Cl(2)	3.450(11)	153
<b>2</b> ·CHCl <sub>3</sub>	C(31)···Cl(2)	3.446(10)	152
<b>1</b> ·( <i>P</i> )–Cl(CH <sub>2</sub> ) <sub>2</sub> Cl	C(31)···Cl(2)	3.695(13)	137
<b>2</b> ·( <i>M</i> )–Cl(CH <sub>2</sub> ) <sub>2</sub> Cl	C(31)···Cl(2)	3.678(14)	134

In both **1**·CH<sub>2</sub>Cl<sub>2</sub> and **2**·CH<sub>2</sub>Cl<sub>2</sub>, the C–H groups from the phenyl ring of the  $\alpha$ -methylbenzylamine fragment (C11–H) of one ligand and the methylene group (C22–H) of the other ligand participate in the C–H···Cl interactions with the Cl atoms (Cl3 and Cl4) of the two adjacent CH<sub>2</sub>Cl<sub>2</sub> molecules. As a result a one-dimensional arrangement of hydrogen bonded alternating dicopper(II) complexes and CH<sub>2</sub>Cl<sub>2</sub> molecules is formed. These chains propagate along the *b* axis and there is a mirror-image relationship between the chains formed by **1**·CH<sub>2</sub>Cl<sub>2</sub> and **2**·CH<sub>2</sub>Cl<sub>2</sub> (Figure 4).

In the case of **1**·CHCl<sub>3</sub> and **2**·CHCl<sub>3</sub>, one of the metal coordinated Cl atoms acts as the acceptor in the C–H···Cl interaction involving the C–H group of the CHCl<sub>3</sub> molecule. These C–H···Cl connected host-guest units, **1**·CHCl<sub>3</sub> and **2**·CHCl<sub>3</sub>, are mirror images of each other (Figure 5). There is no other noncovalent interaction between these discrete host-guest units to form extended networks in the crystal lattice.

The same type of C–H···Cl interaction as observed in **1**·CHCl<sub>3</sub> and **2**·CHCl<sub>3</sub> is present in the cases of **1**·Cl–

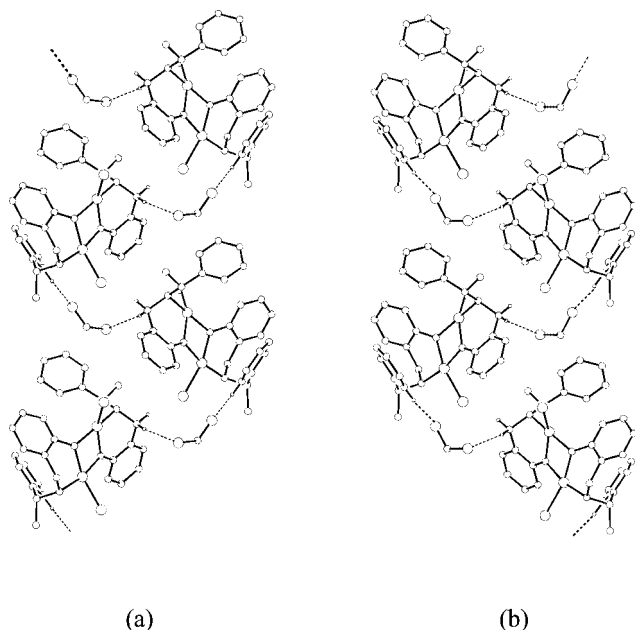


Figure 4. One-dimensional assemblies of (a)  $[\text{Cu}_2\text{L}^1_2\text{Cl}_2] \cdot \text{CH}_2\text{Cl}_2$  (**1**·CH<sub>2</sub>Cl<sub>2</sub>) and (b)  $[\text{Cu}_2\text{L}^2_2\text{Cl}_2] \cdot \text{CH}_2\text{Cl}_2$  (**2**·CH<sub>2</sub>Cl<sub>2</sub>) in the crystal lattice along the *b* axis through C–H...Cl–C interactions; except for the hydrogen atoms of the methylene groups that are involved in intermolecular interactions, all other hydrogen atoms are omitted for clarity.

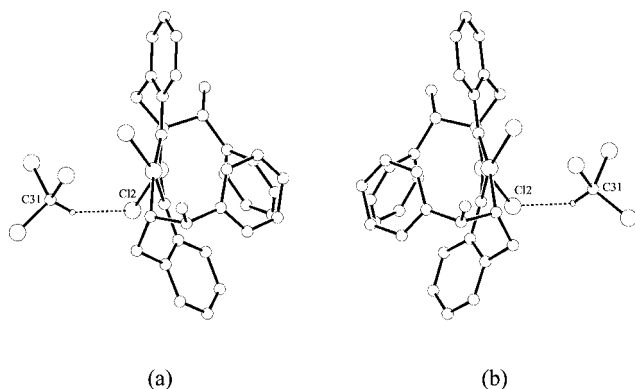


Figure 5. The discrete C–H...Cl–Cu connected (a)  $[\text{Cu}_2\text{L}^1_2\text{Cl}_2] \cdot \text{CHCl}_3$  (**1**·CHCl<sub>3</sub>) and (b)  $[\text{Cu}_2\text{L}^2_2\text{Cl}_2] \cdot \text{CHCl}_3$  (**2**·CHCl<sub>3</sub>) units; hydrogen atoms of **1** and **2** are omitted for clarity.

(CH<sub>2</sub>)<sub>2</sub>Cl and **2**·Cl(CH<sub>2</sub>)<sub>2</sub>Cl. One of the metal coordinated Cl atoms and the C–H group of one of the two methylene groups of Cl(CH<sub>2</sub>)<sub>2</sub>Cl participate in the C–H...Cl interaction. Here as well, no other noncovalent interactions are observed and the crystal lattice contains the discrete C–H...Cl connected host-guest units. Reports on the isolation of the gauche form of Cl(CH<sub>2</sub>)<sub>2</sub>Cl are very rare.<sup>[7,14]</sup> In each of the two present structures, the guest Cl(CH<sub>2</sub>)<sub>2</sub>Cl molecule is in the chiral gauche form. The Cl–C–C–Cl torsion angles are 58(6)° and 50(7)° in **1**·Cl(CH<sub>2</sub>)<sub>2</sub>Cl and **2**·Cl(CH<sub>2</sub>)<sub>2</sub>Cl, respectively. The right-handed or *P* form of the enantiomer is stabilised in the host lattice formed by **1** while the left-handed or *M* form of the enantiomer exists in the host lattice formed by **2** (Figure 6). Thus the chiral host

complexes **1** and **2** produce the appropriate crystal lattices for enantioselective confinement of the chiral *P* and *M* forms of the Cl(CH<sub>2</sub>)<sub>2</sub>Cl rotamers, respectively.

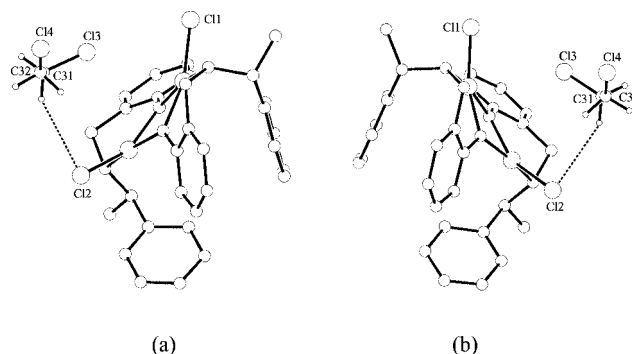


Figure 6. The discrete C–H...Cl–Cu connected (a)  $[\text{Cu}_2\text{L}^1_2\text{Cl}_2] \cdot (P)\text{-Cl}(\text{CH}_2)_2\text{Cl}$  (**1**·(*P*)-Cl(CH<sub>2</sub>)<sub>2</sub>Cl) and (b)  $[\text{Cu}_2\text{L}^2_2\text{Cl}_2] \cdot (M)\text{-Cl}(\text{CH}_2)_2\text{Cl}$  (**2**·(*M*)-Cl(CH<sub>2</sub>)<sub>2</sub>Cl) units; hydrogen atoms of only the Cl(CH<sub>2</sub>)<sub>2</sub>Cl molecules are shown.

## Conclusions

An enantiomeric pair of bisphenoxo-bridged dicopper(II) complexes,  $[\text{Cu}_2\text{L}^1_2\text{Cl}_2]$  (**1**) and  $[\text{Cu}_2\text{L}^2_2\text{Cl}_2]$  (**2**), with the N,O-donor reduced Schiff bases *N*-(2-hydroxybenzyl)-(*R*)- $\alpha$ -methylbenzylamine (HL<sup>1</sup>) and *N*-(2-hydroxybenzyl)-(*S*)- $\alpha$ -methylbenzylamine (HL<sup>2</sup>) have been synthesised and characterised. In each complex, a strong antiferromagnetic spin coupling is operative between the metal centres. Crystallisation efforts revealed that both complexes are excellent hosts for small chloroalkane molecules such as CH<sub>2</sub>Cl<sub>2</sub>, CHCl<sub>3</sub> and Cl(CH<sub>2</sub>)<sub>2</sub>Cl. In all the cases, 1:1 host-guest compounds are formed which crystallise in the noncentrosymmetric space groups. The asymmetric unit of each structure contains a dicopper(II) complex molecule and a guest molecule. The molecular structures of **1** and **2** are mirror images of each other. The NO<sub>2</sub>Cl coordination sphere around each metal centre is distorted from square-planar geometry mainly because of the deviation of the Cl atom from the NO<sub>2</sub> plane. The previously known analogous dicopper(II) complexes are all centrosymmetric and the metal coordinated Cl atoms are trans oriented. In contrast, **1** and **2** are noncentrosymmetric and the Cl atoms are in between the trans and cis orientations. The guest molecules are held in the crystal lattice by intermolecular C–H...Cl interactions. In these interactions, the Cl atom of CH<sub>2</sub>Cl<sub>2</sub> acts as the acceptor while for both CHCl<sub>3</sub> and Cl(CH<sub>2</sub>)<sub>2</sub>Cl the metal coordinated Cl atom acts as the acceptor. Self-assembly of **1**·CH<sub>2</sub>Cl<sub>2</sub> and **2**·CH<sub>2</sub>Cl<sub>2</sub> leads to one-dimensional ordering in the crystal lattice. On the other hand, the crystal lattice contains discrete host-guest units when CHCl<sub>3</sub> or Cl(CH<sub>2</sub>)<sub>2</sub>Cl is the guest. Finally, the rare enantioselective trapping of the chiral rotamers (*P*)-Cl(CH<sub>2</sub>)<sub>2</sub>Cl and (*M*)-Cl(CH<sub>2</sub>)<sub>2</sub>Cl has been realised in the host lattices formed by **1** and **2**, respectively.

## Experimental Section

**Materials:** The chiral reduced Schiff bases (HL<sup>1</sup> and HL<sup>2</sup>) have been synthesised from salicylaldehyde, *R*- or *S*- $\alpha$ -methylbenzylamine and NaBH<sub>4</sub> by following the procedure reported previously.<sup>[5,7]</sup> All other chemicals and solvents were of analytical grade available commercially and were used as received.

**Physical Measurements:** Microanalytical (C, H, N) data were obtained with a Thermo Finnigan Flash EA1112 series elemental analyser. Infrared spectra were collected by using KBr pellets with a Jasco-5300 FT-IR spectrophotometer. A Shimadzu 3101-PC UV/Vis/NIR spectrophotometer was used to record the electronic spectra. Solution electrical conductivities were measured with a Digisun DI-909 conductivity meter. The variable temperature (18–300 K) magnetic susceptibility measurements on powdered samples of **1** were performed using the Faraday technique with a setup comprising a George Associates Lewis coil force magnetometer, a CAHN microbalance and an Air Products closed-cycle helium cryostat. Hg[Co(NCS)<sub>4</sub>] was used as the standard. Diamagnetic corrections calculated from Pascal's constants<sup>[15]</sup> were used to obtain the molar paramagnetic susceptibilities.

### Synthesis of the Complexes

**[Cu<sub>2</sub>L<sup>1</sup>Cl<sub>2</sub>] (1):** A methanol solution (10 mL) of CuCl<sub>2</sub>·2H<sub>2</sub>O (170 mg, 1.0 mmol) was added to a methanol solution (20 mL) of HL<sup>1</sup> (227 mg, 1.0 mmol). The mixture was stirred at room temperature in air for 1 h. The brown solid that separated was collected by filtration, washed with cold methanol (10 mL) and finally dried in air. Yield obtained was 390 mg (60%). C<sub>30</sub>H<sub>32</sub>Cl<sub>2</sub>Cu<sub>2</sub>N<sub>2</sub>O<sub>2</sub> (650.6): calcd. C 55.38, H 4.96, N 4.31; found C 55.45, H 5.02, N 4.20. Electronic spectroscopic data in CHCl<sub>3</sub>:  $\lambda_{\max}$  ( $\epsilon$ ) = 650 sh (345), 430 (3670), 336 sh (2520), 268 nm (12140).

**[Cu<sub>2</sub>L<sup>2</sup>Cl<sub>2</sub>] (2):** This complex was synthesised in 62% yield from HL<sup>2</sup> and CuCl<sub>2</sub>·2H<sub>2</sub>O (1:1 mol ratio) by following the same procedure as described for **1**. It was isolated as a brown solid. C<sub>30</sub>H<sub>32</sub>Cl<sub>2</sub>Cu<sub>2</sub>N<sub>2</sub>O<sub>2</sub> (650.6): calcd. C 55.38, H 4.96, N 4.31; found C 55.24, H 4.92, N 4.26. Electronic spectroscopic data in CHCl<sub>3</sub>: 650 sh (353), 430 (3800), 336 sh (2790), 268 (12530).

**X-ray Crystallography:** X-ray quality crystals of the host-guest species **1**·CH<sub>2</sub>Cl<sub>2</sub>, **2**·CH<sub>2</sub>Cl<sub>2</sub>, **1**·CHCl<sub>3</sub>, **2**·CHCl<sub>3</sub>, **1**·Cl(CH<sub>2</sub>)<sub>2</sub>Cl and **2**·Cl(CH<sub>2</sub>)<sub>2</sub>Cl were grown by slow evaporation of the solutions of

**1** and **2** in the corresponding solvents in air at room temperature (298 K). Unit cell parameters and the intensity data for all the crystals were collected with a Bruker-Nonius SMART APEX CCD single crystal diffractometer, equipped with a graphite monochromator and a Mo-K $\alpha$  fine-focus sealed tube ( $\lambda$  = 0.71073 Å) operated at 2.0 kW. The detector was placed at a distance of 6.0 cm from the crystal. Data were collected at 298 K with a scan width of 0.3° in  $\omega$  and an exposure time of 15 s/frame. The SMART software was used for data acquisition and the SAINT-Plus software was used for data extraction.<sup>[16]</sup> The absorption corrections were performed with the help of the SADABS programme.<sup>[17]</sup> The structures were solved by direct methods and refined on  $F^2$  by full-matrix least-squares procedures. In each structure, all the non-hydrogen atoms were refined using anisotropic thermal parameters. For all the structures, the hydrogen atoms of the metal coordinated secondary amine N atoms were located in the difference Fourier maps and refined isotropically. The rest of the hydrogen atoms in each structure were included in the structure factor calculation at idealised positions by using a riding model, but not refined. The SHELX-97 programmes<sup>[18]</sup> of the WinGX package<sup>[19]</sup> were used for structure solution and refinement. The ORTEP6a<sup>[20]</sup> and Platon packages<sup>[21]</sup> were used for molecular graphics. Selected crystal and refinement data are listed in Table 3.

CCDC-600238 to -600243 contain the supplementary crystallographic data for this paper. These data can be obtained free of charge from The Cambridge Crystallographic Data Centre via [www.ccdc.cam.ac.uk/data\\_request/cif](http://www.ccdc.cam.ac.uk/data_request/cif).

## Acknowledgments

Financial support for this work was provided by the Council of Scientific and Industrial Research (CSIR), New Delhi [Grant No. 01(1880)/03/EMR-II]. V. K. M. thanks the CSIR for a research fellowship. Our sincere thanks go to Prof. A. R. Chakravarty for providing the cryomagnetic data. X-ray crystallographic studies were performed at the National Single Crystal Diffractometer Facility, School of Chemistry, University of Hyderabad (funded by the Department of Science and Technology, New Delhi). We thank the University Grants Commission, New Delhi for the facilities provided under the UPE and CAS programmes.

Table 3. Selected crystallographic data for **1**·CH<sub>2</sub>Cl<sub>2</sub>, **2**·CH<sub>2</sub>Cl<sub>2</sub>, **1**·CHCl<sub>3</sub>, **2**·CHCl<sub>3</sub>, **1**·Cl(CH<sub>2</sub>)<sub>2</sub>Cl and **2**·Cl(CH<sub>2</sub>)<sub>2</sub>Cl.

Compound	<b>1</b> ·CH <sub>2</sub> Cl <sub>2</sub>	<b>2</b> ·CH <sub>2</sub> Cl <sub>2</sub>	<b>1</b> ·CHCl <sub>3</sub>	<b>2</b> ·CHCl <sub>3</sub>	<b>1</b> ·Cl(CH <sub>2</sub> ) <sub>2</sub> Cl	<b>2</b> ·Cl(CH <sub>2</sub> ) <sub>2</sub> Cl
Empirical formula	C <sub>31</sub> H <sub>34</sub> Cl <sub>4</sub> Cu <sub>2</sub> N <sub>2</sub> O <sub>2</sub>	C <sub>31</sub> H <sub>34</sub> Cl <sub>4</sub> Cu <sub>2</sub> N <sub>2</sub> O <sub>2</sub>	C <sub>31</sub> H <sub>33</sub> Cl <sub>5</sub> Cu <sub>2</sub> N <sub>2</sub> O <sub>2</sub>	C <sub>31</sub> H <sub>33</sub> Cl <sub>5</sub> Cu <sub>2</sub> N <sub>2</sub> O <sub>2</sub>	C <sub>32</sub> H <sub>36</sub> Cl <sub>4</sub> Cu <sub>2</sub> N <sub>2</sub> O <sub>2</sub>	C <sub>32</sub> H <sub>36</sub> Cl <sub>4</sub> Cu <sub>2</sub> N <sub>2</sub> O <sub>2</sub>
Formula mass [g·mol <sup>-1</sup> ]	735.5	735.5	769.9	769.9	749.5	749.5
Crystal system	monoclinic	monoclinic	orthorhombic	orthorhombic	orthorhombic	orthorhombic
Space group	<i>P</i> 2 <sub>1</sub>	<i>P</i> 2 <sub>1</sub>	<i>P</i> 2 <sub>1</sub> 2 <sub>1</sub>	<i>P</i> 2 <sub>1</sub> 2 <sub>1</sub>	<i>P</i> 2 <sub>1</sub> 2 <sub>1</sub>	<i>P</i> 2 <sub>1</sub> 2 <sub>1</sub>
<i>a</i> [Å]	8.5479(6)	8.5359(6)	12.7319(6)	12.7250(7)	12.822(3)	12.7982(13)
<i>b</i> [Å]	13.0697(9)	13.0565(10)	13.7805(7)	13.7785(8)	14.046(3)	14.0366(14)
<i>c</i> [Å]	14.1650(9)	14.1597(10)	19.4266(10)	19.4192(11)	18.744(4)	18.7009(19)
$\beta$ [°]	90.941(1)	90.954(1)	90	90	90	90
<i>V</i> [Å <sup>3</sup> ]	1582.28(19)	1577.9(2)	3408.4(3)	3404.8(3)	3375.9(12)	3359.5(6)
<i>Z</i>	2	2	4	4	4	4
$\mu$ [mm <sup>-1</sup> ]	1.713	1.718	1.670	1.672	1.607	1.615
Reflections unique	7370	7305	7958	6928	6517	7860
Reflections [ <i>I</i> > 2 $\sigma$ ( <i>I</i> )]	6813	6744	5909	5521	4934	5870
Parameters	378	378	387	387	387	387
<i>R</i> <sub>1</sub> , <i>wR</i> <sub>2</sub> [ <i>I</i> > 2 $\sigma$ ( <i>I</i> )]	0.0393, 0.1128	0.0403, 0.1162	0.0516, 0.1327	0.0488, 0.1258	0.0475, 0.1151	0.0493, 0.1229
<i>R</i> <sub>1</sub> , <i>wR</i> <sub>2</sub> (all data)	0.0424, 0.1154	0.0432, 0.1187	0.0769, 0.1489	0.0607, 0.1316	0.0727, 0.1242	0.0810, 0.1439
Flack parameter	0.007(12)	0.022(12)	−0.014(17)	−0.029(16)	0.029(17)	−0.001(17)
GOF on $F^2$	1.061	1.056	1.018	0.986	1.047	1.057

- [1] a) X. X. Zhang, J. S. Bradshaw, R. M. Izatt, *Chem. Rev.* **1997**, *97*, 3313; b) M. Munakata, L. P. Wu, T. Kuroda-Sowa, *Adv. Inorg. Chem.* **1999**, *46*, 173; c) K. T. Holman, A. M. Pivovar, M. D. Ward, *Science* **2001**, *294*, 1907; d) F. Toda, *Pure Appl. Chem.* **2001**, *73*, 1137; e) B. Moulton, M. J. Zaworotko, *Chem. Rev.* **2001**, *101*, 1629; f) M. Eddaoudi, D. B. Moler, H. Li, B. Chen, T. M. Reineke, M. O'Keeffe, O. M. Yaghi, *Acc. Chem. Res.* **2001**, *34*, 319; g) O. R. Evans, W. Lin, *Acc. Chem. Res.* **2002**, *35*, 511; h) E. Brunet, *Chirality* **2002**, *14*, 135; i) L. Pérez-García, D. B. Amabilino, *Chem. Soc. Rev.* **2002**, *31*, 342; j) B. Kesaneli, W. Lin, *Coord. Chem. Rev.* **2003**, *246*, 305; k) L. Brammer, *Chem. Soc. Rev.* **2004**, *33*, 476; l) L. Yeo, K. D. M. Harris, *Mendeleev Commun.* **2004**, 263; m) W. Lin, *J. Solid State Chem.* **2005**, *178*, 2486.
- [2] a) *Molecular Nonlinear Optics: Materials, Physics and Devices* (Ed.: J. Zyss), Academic Press, London, **1994**; b) *Handbook of Laser Science and Technology* (Ed.: J. M. Webber), CRC Press, Boca Raton, FL, **1995**.
- [3] a) J. Zyss, J.-F. Nicoud, M. Coquillary, *J. Chem. Phys.* **1984**, *81*, 4160; b) D. E. Eaton, *Science* **1991**, *253*, 281.
- [4] a) F. Averseng, P. G. Lacroix, I. Malfant, F. Dahan, K. Nakatani, *J. Mater. Chem.* **2000**, *10*, 1013; b) S. R. Korupolu, N. Mangayakarasi, S. Ameerunisha, E. J. Valente, P. S. Zacharias, *J. Chem. Soc., Dalton Trans.* **2000**, 2845; c) C. Evans, D. Luneau, *J. Chem. Soc., Dalton Trans.* **2002**, 83.
- [5] V. K. Muppidi, P. S. Zacharias, S. Pal, *Inorg. Chem. Commun.* **2005**, *8*, 543.
- [6] a) J. D. Ranford, J. J. Vittal, D. Wu, *Angew. Chem. Int. Ed.* **1998**, *37*, 1114; b) J. D. Ranford, J. J. Vittal, D. Wu, X. Yang, *Angew. Chem. Int. Ed.* **1999**, *38*, 3498; c) C. T. Yang, B. Moubarak, K. S. Murray, J. D. Ranford, J. J. Vittal, *Inorg. Chem.* **2001**, *40*, 5934; d) J. J. Vittal, X. Yang, *Cryst. Growth Des.* **2002**, *2*, 259; e) S. R. Korupolu, N. Mangayakarasi, P. S. Zacharias, J. Mijuthani, H. Nishihara, *Inorg. Chem.* **2002**, *41*, 4099; f) J. Gao, J. H. Ribenspies, A. E. Martell, *Angew. Chem. Int. Ed.* **2003**, *42*, 6008; g) C. T. Yang, B. Moubarak, K. S. Murray, J. J. Vittal, *Dalton Trans.* **2003**, 880; h) B. Sreenivasulu, J. J. Vittal, *Cryst. Growth Des.* **2003**, *3*, 635; i) M. A. Alam, M. Nethaji, M. Ray, *Angew. Chem. Int. Ed.* **2003**, *42*, 1940; j) C. T. Yang, M. Vetrichelvan, X. Yang, B. Moubarak, K. S. Murray, J. J. Vittal, *Dalton Trans.* **2004**, 113; k) B. Sreenivasulu, J. J. Vittal, *Angew. Chem. Int. Ed.* **2004**, *43*, 5769.
- [7] V. K. Muppidi, P. S. Zacharias, S. Pal, *Chem. Commun.* **2005**, 2515.
- [8] a) H. S. Maslen, T. N. Waters, *Coord. Chem. Rev.* **1975**, *17*, 137; b) S. Das, G. P. Muthukumaragopal, S. N. Pal, S. Pal, *New J. Chem.* **2003**, *27*, 1102; c) S. Das, S. Pal, *J. Mol. Struct.* **2005**, *753*, 68.
- [9] a) S. K. Mandal, L. K. Thompson, M. J. Newlands, E. J. Gabe, K. Nag, *Inorg. Chem.* **1990**, *29*, 1324; b) K. Nag, *Proc. Indian Acad. Sci. (Chem. Sci.)* **1990**, *102*, 269; c) N. R. Sangeetha, K. Baradi, R. Gupta, C. K. Pal, V. Manivannan, S. Pal, *Polyhedron* **1999**, *18*, 1425.
- [10] a) C. M. Harris, E. Sinn, *J. Inorg. Nucl. Chem.* **1968**, *30*, 2723; b) E. Sinn, W. T. Robinson, *J. Chem. Soc., Chem. Commun.* **1972**, 359; c) R. M. Countryman, W. T. Robinson, E. Sinn, *Inorg. Chem.* **1974**, *13*, 2013; d) P. Gluvchinsky, G. M. Mockler, P. C. Healy, E. Sinn, *J. Chem. Soc., Dalton Trans.* **1974**, 1156; e) R. J. Butcher, E. Sinn, *Inorg. Chem.* **1976**, *15*, 1604; f) B. Chiari, O. Piovesana, T. Tarantelli, P. F. Zanazzi, *Inorg. Chem.* **1987**, *26*, 952; g) R. Paschke, S. Liebsch, C. Tschierske, M. A. Oakley, E. Sinn, *Inorg. Chem.* **2003**, *42*, 8230.
- [11] B. Bleany, K. D. Bowers, *Proc. R. Soc. London Ser. A* **1952**, *214*, 451.
- [12] G. V. R. Chandramouli, C. Balagopalakrishna, M. V. Rajasekharan, P. T. Manoharan, *Comput. Chem.* **1996**, *20*, 353.
- [13] a) G. Aullón, D. Bellamy, L. Brammer, E. A. Bruton, A. G. Orpen, *Chem. Commun.* **1998**, 653; b) L. Brammer, E. A. Bruton, P. Sherwood, *Cryst. Growth Des.* **2001**, *1*, 277; c) V. Balamurugan, M. S. Hundal, R. Mukherjee, *Chem. Eur. J.* **2004**, *10*, 1683; d) L. Brammer, *Chem. Soc. Rev.* **2004**, *33*, 476; e) M. Prbhakar, P. S. Zacharias, S. K. Das, *Inorg. Chem.* **2005**, *44*, 2585.
- [14] F. Toda, K. Tanaka, R. Kuroda, *Chem. Commun.* **1997**, 1227.
- [15] W. E. Hatfield, *Theory and Applications of Molecular Paramagnetism* (Eds.: E. A. Boudreaux, L. N. Mulay), Wiley, New York, **1976**, p. 491.
- [16] *SMART V5.630 and SAINT-plus V6.45*, Bruker-Nonius Analytical X-ray Systems Inc., Madison, WI, USA, **2003**.
- [17] G. M. Sheldrick, *SADABS Program for area detector absorption correction*, University of Göttingen, Göttingen, Germany, **1997**.
- [18] G. M. Sheldrick, *SHELX-97 Structure Determination Software*, University of Göttingen, Göttingen, Germany, **1997**.
- [19] L. J. Farrugia, *J. Appl. Crystallogr.* **1999**, *32*, 837.
- [20] P. McArdle, *J. Appl. Crystallogr.* **1995**, *28*, 65.
- [21] A. L. Spek, *PLATON A Multipurpose Crystallographic Tool*, Utrecht University, Utrecht, The Netherlands, **2002**.

Received: March 20, 2006

Published Online: May 12, 2006